International Journal of Chemical Studies

P-ISSN: 2349–8528
E-ISSN: 2321–4902
www.chemijournal.com
IJCS 2021; 9(2): 01-05

Received: 01-01-2021
Accepted: 07-02-2021

Kenneth L Brown
Department of Chemistry, Hope College, Holland, Michigan, USA

Olajide Banks
Department of Chemistry, Hope College, Holland, Michigan, USA

Ana Ortega
Department of Chemistry, Hope College, Holland, Michigan, USA

Bruce Kraay
Department of Chemistry, Hope College, Holland, Michigan, USA

Corresponding Author:
Kenneth L Brown
Department of Chemistry, Hope College, Holland, Michigan, USA

Preparation and cyclic Voltammetric characterization of three-dimensional macroporous carbon electrodes

Kenneth L Brown, Olajide Banks, Ana Ortega and Bruce Kraay

DOI: https://doi.org/10.22271/chemi.2021.v9.i2a.11841

Abstract
Three-Dimensionally Ordered Macroporous (3DOM) carbon surfaces were prepared from a template synthesis involving polymethyl methacrylate. These surfaces were mounted as electrodes and studied using cyclic voltammetry to understand their electrochemical properties for potential use as platforms in electrochemical sensors. The prepared 3DOM carbon electrodes have a large surface area that allows more charge-transfer reactions to take place. Potassium hexacyanoferrate and potassium nitrate served as the electroactive species and supporting electrolyte, respectively to study the 3DOM electrodes. Based on the Randles-Sevcik equation, the current produced by the potassium hexacyanoferrate electroactive species, is controlled by diffusion. The electrodes were subsequently chemically modified with 13 nm gold nanoparticles that produced a significant increase in the faradaic current.

Keywords: Cyclic voltammetry, three-dimensionally ordered microporous electrodes, diffusion

Introduction
Throughout the past decade, research has been done using three dimensionally ordered macroporous (3DOM) electrodes. The defining feature of 3DOM carbon electrodes is the ordered array of spherical void macropores surrounded by a carbon backbone. The macropores are interconnected by small micropores present within the carbon backbone. According to researchers this arrangement allows for large surface areas up to 670 m^2/g and specific capacitances of 150 g/F when fabricated for electrochemical use [1]. The porous nature and large surface area of 3DOM have attracted researchers to study its use in a variety of applications. One main focus has been in the improvement of Li ion batteries [2-3]. The porous structure leads to shorter diffusion lengths and an increase in the number of active sites at which charge transfer reactions can occur. Hence, numerous studies have attempted to increase the effectiveness of Li ion batteries through the use of 3DOM carbon. A large number of oxides have shown increased capacitive abilities when coated onto the surface of the carbon [4]. Another area of ongoing research is the use the 3DOM carbon for solid contact ion selective electrodes. Ultra-low detection limits of Ag^+ and K^+ have been reported for ion selective electrodes using 3DOM as the solid contact [5]. Other studies have shown that these electrodes have good long-term potential stability as reference electrodes [6]. Cyclic voltammetry is a versatile method used to characterize electrochemical systems. This method has been used to prepare organic conducting polymers and metals coatings, determine redox properties such as formal reduction potentials, and perform spectroelectrochemical measurements [7-15]. In this paper, we describe the preparation of the 3DOM carbon-based electrodes and report on the electrochemical properties of 3DOM carbon electrodes using cyclic voltammetry to aid in future studies involving these electrode platforms towards developing biosensors.

Materials and Methods
Instrumentation
All cyclic voltammetry experiments were performed using a Pine Research potentiostat and Aftermath software (North Carolina). A three-electrode electrochemical cell consisting of a saturated Ag/AgCl, 3 M NaCl reference electrode, an auxiliary platinum wire mesh electrode, and 3DOM carbon working electrode was used for all electrochemical measurements.

Scanning electron microscope images of the 3DOM carbon surfaces were obtained with a Hitachi TM3000 table top scanning electron microscope using an electron beam strength of 15 kV.

Electrochemical measurement parameters and solutions

The electrolytic solution used for cyclic voltammetry measurements was 1.00 x 10^{-3} mol·L^{-1} $K_3Fe(CN)_6$ as the electroactive species and 0.10 M KNO_3 as the supporting electrolyte. The solutions were prepared using water purified by reverse osmosis. Nitrogen gas was bubbled into the solutions for at least five minutes before all electrochemical experiments and a nitrogen blanket was maintained over the solution during the measurements. The potential window was 1.00 V to -0.400 V with scan rates of 10-100 mV·s^{-1}.

3DOM electrode fabrication

The 3DOM platforms were prepared using colloidal crystal templating of polymethyl methacrylate (PMMA) spheres with no deviations from the literature procedures [21]. After synthesizing the PMMA, the solution was left to dry for forty-five days. Then, a resorcinol formaldehyde precursor solution was added to a small batch of dried PMMA template and left to age for 3 days at 85 ºC. Finally, the PMMA template, saturated with the resorcinol formaldehyde solution, underwent a carbonization process at 700 ºC in an inert argon atmosphere. The 3DOM electrodes were polished on a wetted 600 grit sandpaper by applying a gentle pressure. This was followed by sonicating the 3DOM carbon electrode repeatedly and rinsing the electrode until all traces of carbon powder were removed. The electrodes were placed on top of a vacuum filtration apparatus for 15 minutes, followed by drying in an oven at 110 °C for two hours. The dried 3DOM carbon electrode was mounted to Ni mesh using a prepared glue solution containing 0.0150 g sodium carbonate and 0.8250 g resorcinol in 1.13 mL formaldehyde. Sodium bicarbonate was dissolved in formaldehyde after which the resorcinol was added and stirred for 20 minutes. The solution was heated to 40 °C for 15 minutes and then the heat was increased to 55 °C. The 3DOM electrode was placed in an oven at 110 °C to harden the glue. Afterwards, the 3DOM carbon electrode with the attached Ni mesh was sandwiched between two sheets of PVC such that all of the Ni mesh was covered except for a small bit on the opposite end. Figure 1 (a-c) shows an overview of the three-step construction of the electrode.

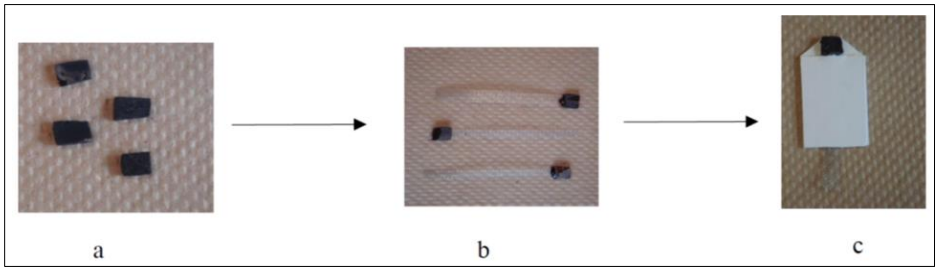

Fig 1: Preparation of electrode. Overview of the 3DOM electrode development process. a. 3DOM surface after carbonization from precursor solution. b. Mounting of the electrode to the nickel wire mesh. c. 3DOM electrode covered with PVC sheet

Gold nanoparticle treatment of the 3DOM carbon electrode

Gold nanoparticles were synthesized by a Frens citrate reduction [17]. Aqua regia, followed by distilled water, was used to rinse all glassware prior to use. Sodium citrate (38.8 mM), in the amount of 25.00 mL was added to an aqueous solution of potassium Tetrachloroaurate(III) dihydrate under a stirred reflux. After which, the solution changed from pale yellow to dark red and was refluxed for an additional 15 minutes. The solution was allowed to cool to room temperature prior to using them to modify the 3DOM electrode. The surface of the 3DOM carbon electrode was modified by placing the 3DOM carbon in 20 mL of gold nanoparticle solution and sonicating for 1 hour, followed by placing the electrode in the oven for one hour to dry. Another method consisted of drop-coating the 3DOM electrode in the nanoparticle solution. The TM3000 along with BRUKER XFlash MIN SVE, BRUKER Scan Generator and Quantax 70 software was used for elemental analysis via electron energy dispersive X-ray spectrometry (EDS). A Cary 50 UV-Visible double-beam spectrometer (Varian) was used to obtain a spectrum of the gold nanoparticles.

Results and Discussion

SEM characterization of the 3DOM carbon electrode

The colloidal crystal templating of poly(methyl methacrylate) spheres facilitated the synthesis of 3DOM carbon electrode. The evenly distributed array of void spaces resulted in green and blue colors being visible on the surface of the 3DOM carbon electrode when viewed with the naked eye. Such opalescence arises due to the diffraction of light through the uniform distribution of the pores. The blue/green color observed is directly related to the size of the pores wherein the pore size is on the same order as the wavelength of light. Scanning electron microscopy imaging shown in Figure 1 reveals the porous nature of the 3DOM carbon electrode with an average pore size of 283±15 nm. This pore size agrees with previously reported colors and pore sizes [1]. Using EDS, the relative amount of gold, potassium, and sodium incorporated into the surface of the 3DOM electrode from the two nanoparticle immobilization methods was determined as shown in Table 1. For these three elements, the sonication method yields lower amounts of gold, potassium and sodium incorporated onto the 3DOM electrode surface. No doubt the sonication method results in the removal of the gold nanoparticles that were originally incorporated onto the 3DOM electrode surface. Therefore, the drop-coating method was used to modify the 3DOM electrode surface for the electrochemical studies discussed later.

Table 1: Summary of gold nanoparticle immobilization. Elemental composition of 3DOM carbon surface after nano-particle immobilization scheme. Two methods were used for immobilization of nanoparticles

Element	Sonication	Drop-coating
Gold (Au)	139	9847
Potassium (K)	122	5058
Sodium (Na)	229	24423

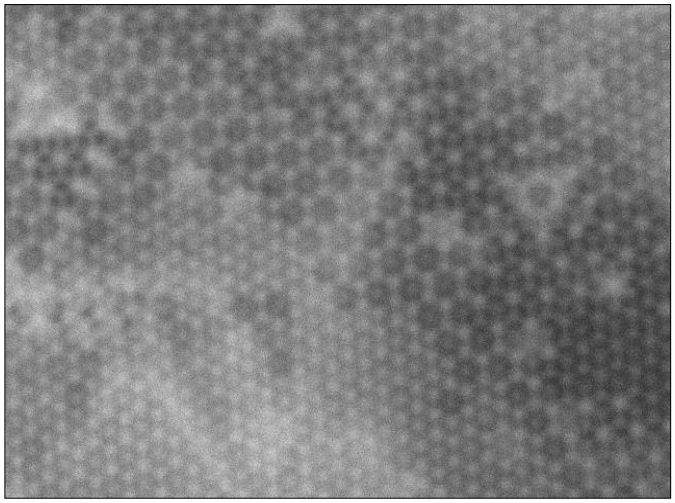

Fig 2: Scanning electron microscopy image of 3DOM carbon at 30,000X magnification that shows the ordered array of spherical void spaces present in the electrode

Electrochemical characterization

The results from cyclic voltammetry measurements provide insight into the performance of the 3DOM carbon as a working electrode in three-electrode electrochemical cell. Figure 2 shows cyclic voltammograms at various scan rates from 10 -100 $mV{\cdot}s^{-1}$. At a low scan rate of 10 $mV{\cdot}s^{-1}$, the peak separation (ΔEp) is 0.089 V, but then increases to 0.180 V when the scan rate increases to 100 $mV{\cdot}s^{-1}$; the ratio of the peak currents (i_{pc}/i_{pa}) varies from 0.97 to 1.21. Both of these parameters indicate that the electrochemistry of $K_3Fe(CN)_6$ becomes more quasireversible using the 3DOM electrode. The formal reduction potential, E°', varies from 0.262 V to 0.260 V and was determined using $(E_{pa}+ E_{pc})/2$, where E_{pa} and E_{pc} are the anodic and cathodic peak potentials, respectively.

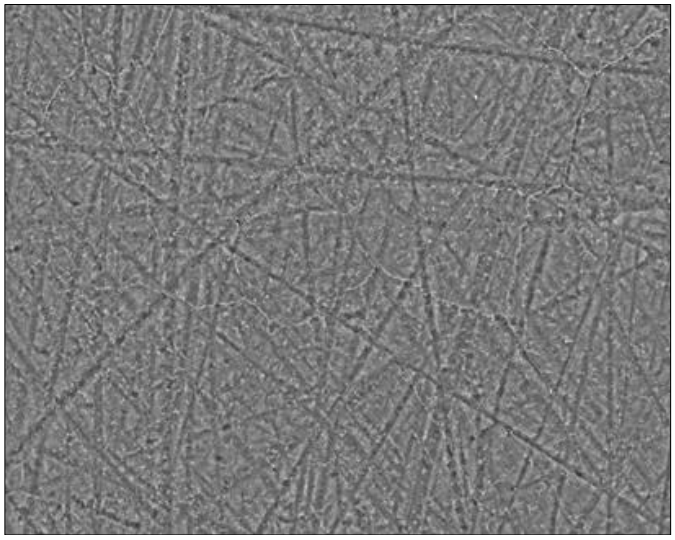

Fig 3: Scanning electron microscopy image of 3DOM carbon at 250X magnification

Plots of the peak current relative to the square root of the scan rate produce linear trends as shown in Figure 4, indicating diffusion-controlled conditions as given by the Randles-Sevcik equation (Eq. 1), where the symbols have their normal electrochemical convention.

$$i_p = 2.69 \times 10^5 n^{3/2} A D^{1/2} C v^{1/2} \quad \text{(Eq. 1)}$$

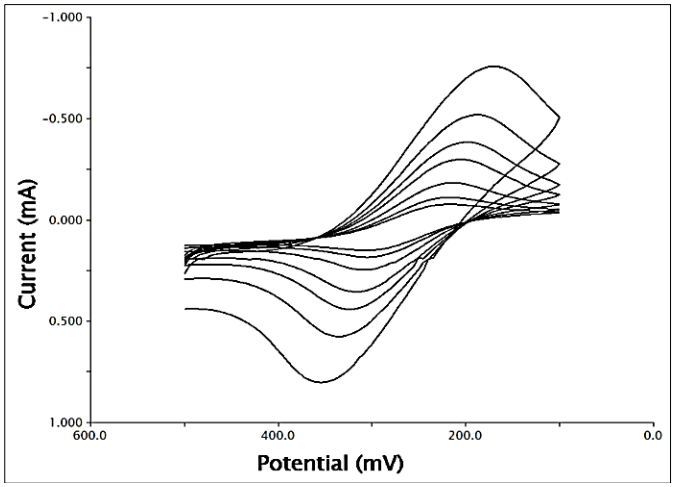

Fig 4: Overlay of various scan rates cyclic voltammograms from 10 $mV{\cdot}s^{-1}$ to 100 $mV{\cdot}s^{-1}$. Solution consists of 1.00 x 10^{-3} $mol{\cdot}L^{-1}$ $K_3Fe(CN)_6$ in 0.10 $mol{\cdot}L^{-1}$ KNO_3. 3DOM working electrode, Ag/AgCl reference electrode, and platinum auxiliary electrode. Dimensions of the electrode were 3 mm x 2 mm x 1 mm (*length x width x height*)

A similar study reported on the diffusion of $K_3Fe(CN)_6$ to an electrode consisting of carbon nanotube bundles. They reported heavily overlapping diffusion layers at each carbon nanotube, which resulted in semi-infinite planar diffusion similar to diffusion at planar macroelectrodes [16].

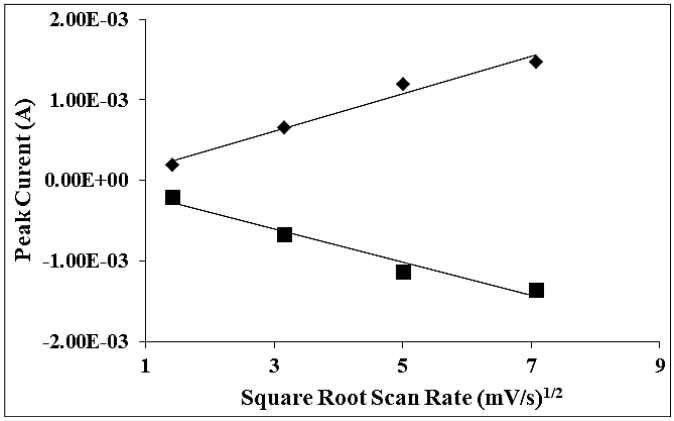

Fig 5: Diffusion controlled conditions graph. Graph showing the relationship between current and the square root of the scan rate at scan rates of 5 to 50 $mV{\cdot}s^{-1}$ with 1.00 x 10^{-3} $mol{\cdot}L^{-1}$ $K_3Fe(CN)_6$ using 3DOM working electrode, Ag/AgCl reference electrode, and platinum auxiliary electrode in 0.10 $mol{\cdot}L^{-1}$ KNO_3

In Figure 5, the equation of line reflective of the reduction process is y = 0.0002x-9x10^{-5} and for oxidation process, the equation of the line is y= -0.0002x-2 x10^{-5}. Due to the pores present within the 3DOM carbon electrode, diffusion of the electroactive species resembles carbon nanotube bundle electrodes. At each pore of the 3DOM electrode, overlapping diffusion layers serve to channel electroactive species to the inner surfaces of the electrode. At higher scan rates (e.g., 100 $mV{\cdot}s^{-1}$) only part of the electrode surface area is accessible for the Fe(III)/Fe(II) redox couple during the time scale of the cyclic voltammogram, and therefore diffusion of the electroactive species to the inner pore surface area may become limited; with a large surface area confined within the pores, diffusion to the innermost parts of the pores may be limited and difficult to achieve. The relationship between

peak separation and the scan rate indicates a quasireversible system that is dependent upon the electron transfer kinetics between the Fe(III)/Fe(II) redox sites and the 3DOM electrode surface. Both the peak separation and the i_{pc}/i_{pa} values deviate from the idea values of 59 mV and 1.00, respectively for a reversible system. Figure 4 shows that the anodic and cathodic peak currents increase with higher concentrations of $K_3Fe(CN)_6$, thus producing a trend that follows Eq. 1 over a range of 0 mol·L^{-1} to 0.100 mol·L^{-1}; in Figure 4, scan rates of 2, 10, and 25 mV·s^{-1} were used. The different slopes of the lines reflect the various scan rates used for the reduction process, Fe^{3+} + e- →Fe^{2+}, wherein the slopes corresponding to 2, 10, and 25 mV·s^{-1} are 0.0283, 0.0638 and 0.0970, respectively, and they reflect the square root dependence on the scan rates.

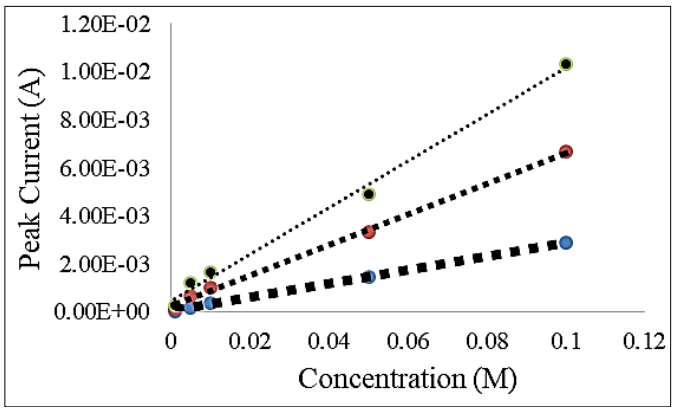

Fig 6 Current-Concentration profile. Graph showing the relationship between current and concentration (0-0.10 mol·L^{-1}) at scan rates of 2, 10, and 25 mV·s^{-1} from 0 - 0.1 mol·L^{-1} $K_3Fe(CN)_6$ using 3DOM working electrode, Ag/AgCl reference electrode, and platinum auxiliary electrode in KNO_3.

The surface of the 3DOM electrode was modified with gold nanoparticles (GN) using a drop-coating method. A UV-Vis spectrum of the gold nanoparticles in Figure 7 shows a peak at 520 nm indicating the presence of the GN; the peak at 520 nm is a result of the surface plasmon resonance. The presence of the GN alters not only the surface area but also the surface energy density of the 3DOM material. Immobilization of the GN onto the surface and within the pores of the 3DOM electrodes yields a significant enhancement of the peak currents with more than a ten-fold increase as shown in Figure 8. However, the peak separation increases by c.a. 0.200 V when compared to electrodes with no immobilized gold nanoparticles.

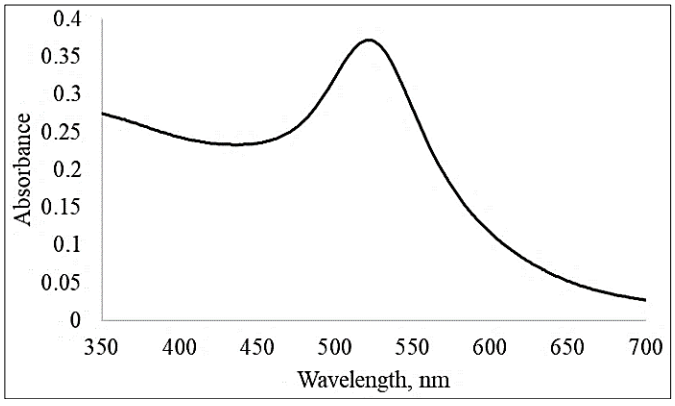

Fig 7: Spectrum profile of gold nanoparticles. Spectrum from 350 nm-700 nm in a 1-cm cuvette of gold nanoparticles showing an absorbance maximum at 520 nm

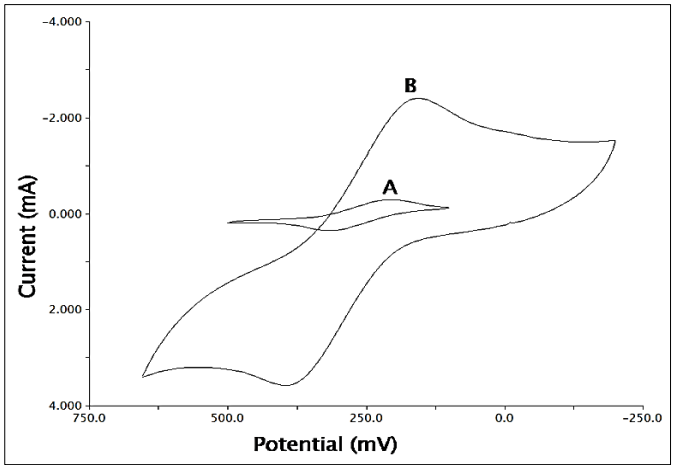

Fig 8: Cyclic voltammogram of 1.00 x 10^{-3} M $K_3Fe(CN)_6$ in 0.10 M KNO_3 with a) 3DOM working electrode and b) 3DOM working electrode with immobilized gold nanoparticles. Both A and B: Ag/AgCl reference electrode, and platinum auxiliary electrode at 20 mV·s $^{-1}$

Electrochemical impedance spectroscopy measurements were made using frequencies 0.01-50000 Hz at 0.300 V to better understand and differentiate the mass and charge transfer processes at the 3DOM surfaces. The overall impedance of the 3DOM porous electrode is a composite of two processes: the charge transfer impedance of reactions within the pores and the mass transfer impedance within the pores. However, Figure 7 shows a Nyquist plot that has a negligible charge transfer impedance. The diagonal line at low frequencies (i.e., <0.40 Hz) yields a phase angle of -45º for a Warburg mass transfer impedance.

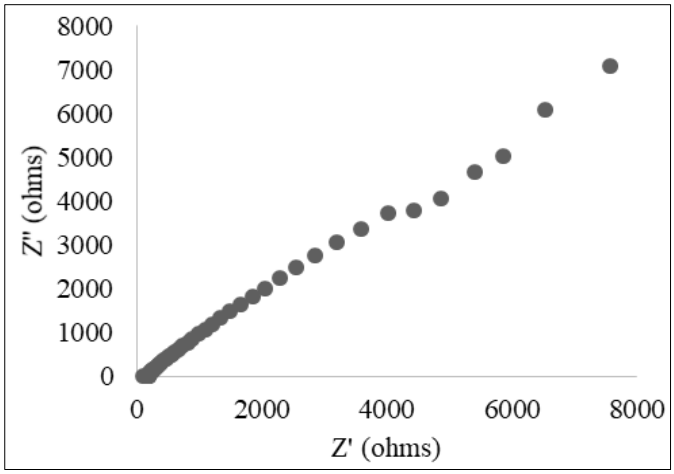

Fig 9: Electrochemical impedance spectrum. A nyquist plot show the warburg impedance for a diffusion-based process using 1.00 x 10^{-3} M $K_3Fe(CN)_6$ in 0.10 M KNO_3 with 3DOM working electrode, Ag/AgCl reference electrode, and platinum auxiliary electrode at 10 mV·s $^{-1}$. The DC potential is 0.300 V with an AC component of 0.010 V from 0.01- 50,000 Hz

Only a fraction of the porous structure is accessible for diffusion, and therefore, only a portion of the porous structure is available for capacitive double layer charging. The overall impedance is dependent upon the geometry of the pores, penetration depth of the electroactive species and ions, and the size distribution of *n* number of pores.

Conclusion

The 3DOM electrode platforms were prepared using colloidal crystal templating of polymethyl methacrylate (PMMA)

spheres. The electrochemistry of the electroactive species, $K_3Fe(CN)_6$, shows quasireversible behaviour using the 3DOM carbon electrodes. One of the key features of these electrodes is the porous network distributed across the surface of the electrode that facilitates the mass transport process of diffusion. Cyclic voltammetry measurements demonstrated that currents produced in the three-electrode electrochemical cell follow the Randles-Sevick equation, thus verifying a diffusion-controlled process; in addition, the peak currents are proportional to the concentration of the electroactive species. A significant increase in the faradaic current was observed during cyclic voltammetric characterization when the gold nanoparticles were immobilized onto the 3DOM electrode surface. These results show that the 3DOM electrode surfaces can be used in three-electrode electrochemical cell and chemically modified to alter the properties of the 3DOM electrode surface. Further research is being conducted to determine how these electrodes will perform in sensor and biosensor applications.

Acknowledgements
This work was funded by the National Science Foundation: NSF-REU Grant #0851194 and NSF-URC Grant #0629174.

References

1. Lee KT, Lytle JC, Ergang NS, Oh SM, Stein A. Synthesis and rate performance of monolithic microporous carbon electrodes for lithium-ion secondary batteries. Adv. Funct. Mater 2005;15(4):547-556.
2. Vu A, Li X, Phillips J, Han A, Smyrl WH, Bühlmann P, Stein A. Three-dimensionally ordered microporous (3Dom) carbon materials as electrodes for electrochemical double-layer capacitors with ionic liquid electrolytes. Chem. Mater 2013;25(21):4137-4148.
3. Hu YS, Adelhelm P, Smarsly BM, Hore S, Antonietti M, Maier J. Synthesis of hierarchically porous carbon monolithic with highly ordered microstructure and their application in rechargeable lithium batteries with high-rate capability. Adv. Funct. Mater 2007;17(12):1873-1878.
4. Wang Z, Li F, Ergang NS, Stein A. Chem. Mater. Effects of hierarchical architecture on electronic and mechanical properties of nanocast monolithic porous carbon and carbon-carbon nanocomposites 2006;18(23):5543-5553.
5. Lai CZ, Joyer MM, Fierke MA, Petkovich ND, Stein A, Bühlmann P. Subnanomolar detection limit application of ion-selective electrodes with three-dimensionally ordered microporous (3DOM) carbon solid contacts. J Solid State Electrochem 2009;13(1):123-128.
6. Zhang T, Lai C-Z, Fierke MA, Stein A, Bühlmann P. Advantages and limitations of reference eletrodes with an ionic liquid junction and three-dimensionally ordered microporous carbon as solid contact. Anal. Chem 2012;84(18):7771-7778.
7. Bettelheim A, White BA, Raybuck SA, Murray RW. Electrochemical Polymerization of Amino-, Pyrrole-, and Hydroxy-Substituted Tetraphenylporphyrins. Inorg. Chem 1987;26(7):1009-17.
8. Dorman SC, Harrington JP, Martin MS, Johnson TV. Determination of the Formal Reduction Potential of Lumbricus Terrestris Hemoglobin Using Thin Layer Spectroelectrochemistry. J Inorg. Biochem 2004;98(1):185–88.
9. Lindholm B. Ac-Impedance Studies of Charge Transport and Redox Capacities at Poly-4-Vinylpyridine Films on Electrode Surfaces. J Electroanal. Chem. Inter. Electrochem 1990;289(1–2):85–101.
10. Heinze J. Cyclic Voltammetry—'Electrochemical Spectroscopy'. New Analytical Methods (25). Angewandte Chemie International Edition in English 1984;23(11):831–47.
11. Cinti S, Mazzaracchio V, Cacciotti I, Moscone D, Arduini F. Carbon Black-Modified Electrodes Screen-Printed onto Paper Towel, Waxed Paper and Parafilm M®. Sensors 2017;17(10):2267.
12. Elgrishi N, Rountree KJ, McCarthy BD, Rountree ES, Eisenhart TT, Dempsey JL. A Practical Beginner's Guide to Cyclic Voltammetry. J Chem. Educ 2018;95(2):197–206.
13. D'Antonio EL, Bowden EF, Franzen S. Thin-Layer Spectroelectrochemistry of the Fe(III)/Fe(II) Redox Reaction of Dehaloperoxidase-Hemoglobin. J Electroanal. Chem 2012;668:37–43.
14. Yu Y, Zhou M, Cui H. Synthesis and Electrochemiluminescence of Bis(2,2′-Bipyridine)(5-Amino-1,10-Phenanthroline) Ruthenium(II)-Functionalized Gold Nanoparticles. J Mater. Chem 2011;21(34):12622–25.
15. Brown KL, Danforth R, Bleitz E, Hwang Y, Rens D. Cyclic Voltammetric and Spectroelectrochemical Studies of Tris(5-amino-1,10-Phenanthroline)Iron(II) Polymer Films. Int. J Electrochem. Sci 2020;15:10707–10721.
16. Fierke MA, Lai C, Buhlmann P, Stein A. Effects of architecture and surface chemistry of three-dimensionally ordered macroporous carbon solid contacts on performance of ion-selective electrodes. Anal. Chem 2010;82:680-688.
17. Frens G. Controlled nucleation for the regulation of the particle size in mondisperse gold suspensions. Nat. Phys. Sci 1973;241:20-22.